Journal of Power Sources 195 (2010) 1446–1453

Contents lists available at ScienceDirect

Journal of Power Sources

journal homepage: www.elsevier.com/locate/jpowsour

Effects of fuel processing methods on industrial scale biogas-fuelled solid oxide fuel cell system for operating in wastewater treatment plants

Siamak Farhad [a], Yeong Yoo [b], Feridun Hamdullahpur [c,*]

[a] Department of Mechanical & Aerospace Engineering, Carleton University, 1125 Colonel By Dr. Ottawa, ON, Canada K1S 5B6
[b] Institute for Chemical Process and Environmental Technology, National Research Council of Canada, 1200 Montreal Rd., Ottawa, ON, Canada K1A 0R6
[c] Department of Mechanical & Mechatronics Engineering, University of Waterloo, 200 University Avenue, West Waterloo, ON, Canada N2L 3G1

ARTICLE INFO

Article history:
Received 19 July 2009
Received in revised form
11 September 2009
Accepted 14 September 2009
Available online 20 September 2009

Keywords:
Solid oxide fuel cell
CHP system
Biogas
Wastewater treatment plant
Fuel processor

ABSTRACT

The performance of three solid oxide fuel cell (SOFC) systems, fuelled by biogas produced through anaerobic digestion (AD) process, for heat and electricity generation in wastewater treatment plants (WWTPs) is studied. Each system has a different fuel processing method to prevent carbon deposition over the anode catalyst under biogas fuelling. Anode gas recirculation (AGR), steam reforming (SR), and partial oxidation (POX) are the methods employed in systems I–III, respectively. A planar SOFC stack used in these systems is based on the anode-supported cells with Ni–YSZ anode, YSZ electrolyte and YSZ–LSM cathode, operated at 800 °C. A computer code has been developed for the simulation of the planar SOFC in cell, stack and system levels and applied for the performance prediction of the SOFC systems. The key operational parameters affecting the performance of the SOFC systems are identified. The effect of these parameters on the electrical and CHP efficiencies, the generated electricity and heat, the total exergy destruction, and the number of cells in SOFC stack of the systems are studied. The results show that among the SOFC systems investigated in this study, the AGR and SR fuel processor-based systems with electrical efficiency of 45.1% and 43%, respectively, are suitable to be applied in WWTPs. If the entire biogas produced in a WWTP is used in the AGR or SR fuel processor-based SOFC system, the electricity and heat required to operate the WWTP can be completely self-supplied and the extra electricity generated can be sold to the electrical grid.

1. Introduction

Biogas gas is a renewable and alternative fuel that can assist to reduce the consumption of fossil fuel and emission of greenhouse gases. Pressure from environmental legislations on solid waste disposal methods in developed countries has increased the application of the anaerobic digestion (AD) process in wastewater treatment plants (WWTPs) for reducing waste volumes and generating useful by-products. One of the important by-products of this process is a biogas containing mainly methane and carbon dioxide, suitable for on-site heat and electricity generation required for the AD process.

Fuel cells convert the chemical energy of a fuel to electricity with high efficiency and they are promising power generation devices to use biogas as a fuel [1–5]. In the United States, if fuel cells are applied to convert biogas, generated in WWTPs, to electricity, there is potential to provide around 2 GW of electricity; the world-wide potential is approximately 13 GW [6]. The first project of this type was undertaken in California in 1999. The plant converted around 3400 m^3 of methane gas produced daily into hydrogen, fuelling two 200 kW phosphoric acid fuel cells to generate electricity and heat. The fuel cells provided 75–90% of the facility's electricity and the heat required for the digester, resulting in combined heat and power (CHP) efficiency between 80% and 90% [7]. The first European fuel cell-based system was developed in Germany in 2005. In this project, a 250 kW molten carbonate fuel cell provided the power and heat required for the WWTP using around 1500–2000 m^3 biogas produced per day [8].

Solid oxide fuel cell (SOFC) has significant advantages of fuel flexibility and high electrical and overall efficiencies. It can achieve a satisfactory performance even using biogas directly without the need for external hydrogen conversion [9–13]. Yi et al. showed that the electrical efficiency of an integrated SOFC system drops only around 1.1% once biogas with 60% methane and 40% carbon dioxide is used instead of natural [14]. In this paper, the performance of SOFC systems fuelled with biogas produced through AD process, with anode gas recirculation, external steam reforming, and partial oxidation, to supply electricity and heat required for WWTPs is studied.

* Corresponding author. Tel.: +1 519 888 4467; fax: +1 519 885 5862.
E-mail addresses: fhamdull@uwaterloo.ca, siamak_farhad@yahoo.com (F. Hamdullahpur).

0378-7753/$ – see front matter.
doi:10.1016/j.jpowsour.2009.09.032

2. Biogas produced in WWTPs

In AD process, micro-organisms break down biodegradable materials in the absence of oxygen. Typically, this process begins with hydrolysis of the inlet materials to break down insoluble organic polymers to make them available to other bacteria. Acidogenic bacteria then convert the amino acids and sugars into hydrogen, carbon dioxide, ammonia, and organic acids. Furthermore, acetogenic bacteria convert the organic acids into acetic acid, along with additional hydrogen, carbon dioxide and ammonia. Methanogens finally convert these products to carbon dioxide and methane, which are the main constituent compounds of the biogas [15–17]. The AD process takes place over a wide range of temperatures from 10 to over 100 °C [18].

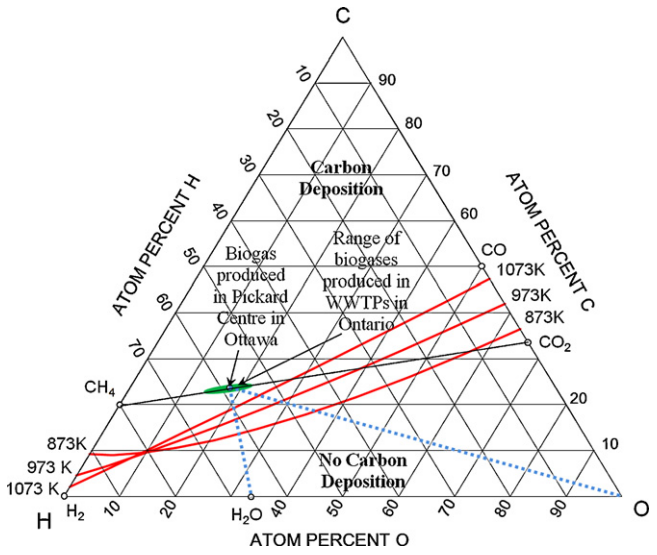

Fig. 1. The location of biogases produced in WWTPs in Ontario and carbon deposition boundary curves in the C–H–O ternary diagram.

Table 1
Biogas composition from WWTPs in Ontario [14].

Compound	Average	Range
CH_4 (%)	60.8	58–70
CO_2 (%)	34.8	30–43
O_2 (%)	1.5	0.1–2
N_2 (%)	2.4	1.2–7.1
H_2O (%)	0.01	0.01
H_2S (ppm)	570	2.5–3450
CO (ppm)	<100	0–100
H_2 (ppm)	<100	0–100
Silicon compounds (ppm)	n/a	0–2500

At present, a significant number of WWTPs in the province of Ontario in Canada employ the AD process and approximately 314,000 m^3 of biogas is produced per day. A majority of the AD-generated biogas in Ontario is simply flared off into the atmosphere [19]. Table 1 lists the key chemical species in the biogas produced from WWTPs in Ontario. Other compounds such as toluene, benzene, methyl chloride, and CFCs are present at levels below 10 ppm. The relative percentage of these gases in the biogas depends on the feed material and control of the process. The outlet temperature and pressure of the biogas are typically 30 °C and near atmospheric pressure, respectively [19].

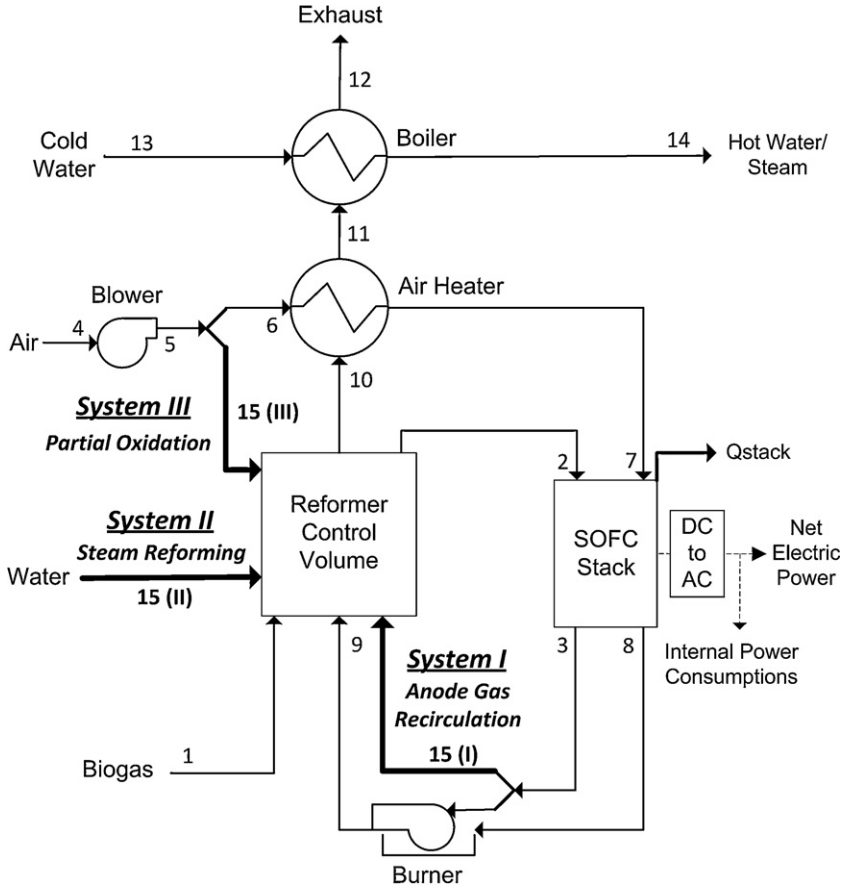

Fig. 2. Configuration of the biogas-fuelled SOFC systems (system I with anode gas recirculation, system II with steam reforming, and system III with partial oxidation reformer).

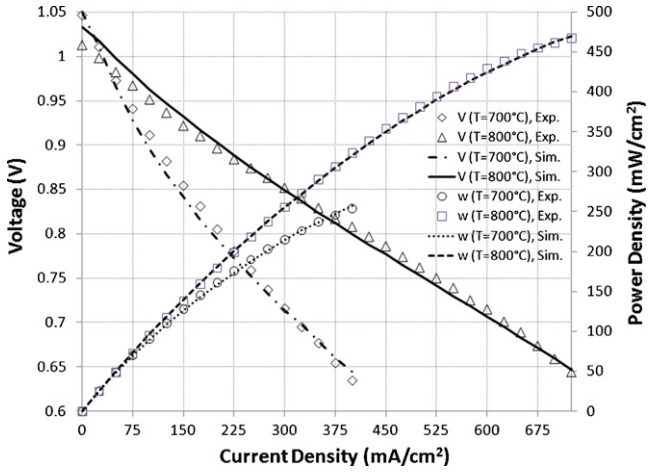

Fig. 3. Results of the computer simulation and experiment for ASC 3 cells.

Table 2
Input data for computer simulation of the anode-supported SOFC cell.

Parameter	Value
Operating voltage	0.7 V
Operating temperature	800 °C
Operating pressure	1 atm
Fuel utilization ratio	80%
Anode	
Thickness	518 μm
Porosity	0.33 (–)
Tortuosity	4 (–)
Cathode	
Thickness	45 μm
Porosity	0.33 (–)
Tortuosity	4 (–)
Electrolyte thickness	5 μm
Interconnect thickness	3 mm
Cell active length	10 cm
Cell active width	10 cm

The composition of biogases produced from WWTPs in Ontario and carbon deposition boundary curves at different temperatures of 873, 973, and 1073 K under atmospheric pressure are shown in the C–H–O ternary diagram in Fig. 1. According to this figure, the composition of the biogases is located above the carbon deposition boundary curves, indicating carbon deposition may occur over the anode catalyst. Carbon deposition deactivates the anode catalyst for the electrochemical and chemical reactions in anode and reduces the performance of the SOFC stack gradually [20–25]. Therefore, appropriate fuel processing in a biogas-fuelled SOFC system should be considered to prevent this coking problem. The steam reforming (SR) [26–28], partial oxidation (POX) [29,30], auto-thermal reforming [31,32], and anode gas recirculation (AGR) [33,34] are typical fuel processing methods in hydrocarbon gas-fuelled SOFC systems.

Table 3
Input data for computer simulation of the SOFC stack.

Parameter	Value
Insulation	
Thickness	50 mm
Thermal conductivity	0.025 W m^{-1} K^{-1}
Emissivity of the outer metal surface	0.8 (–)
Fuel inlet temperature	700 °C
Air inlet temperature	700 °C

Table 4
Input data for computer simulation of SOFC systems.

Parameter	Value
Biogas volumetric flow rate	27,000 m^3 day^{-1}
Biogas composition	CH_4 = 61%
	CO_2 = 37.4%
	N_2 = 1.2%
	H_2S = 6.5 ppm
Pressure drop	0.3 bar
Air blower efficiency	62.5%
Inlet cold water temperature	35 °C
Outlet hot water temperature	95 °C
Inverter efficiency	92%
Flue gas exhaust temperature	$T_{dewPoint}$ + 50 °C
Pinch temperature in boiler	>20 °C

3. Configuration of the SOFC systems

Three configurations related to fuel processing in a biogas-fuelled SOFC system are evaluated for operation in a WWTP. As shown in Fig. 2, these systems are mainly comprised of an SOFC stack to produce DC electricity and heat; an air heater to increase the air temperature before entering the SOFC stack; an air blower to overcome the pressure drop in the system; a burner to convert the chemical energy of the unutilized fuel in the SOFC stack to heat; a boiler to supply the thermal energy required for the AD process and space heating in buildings; an inverter to convert the generated DC electricity to AC; and a reformer control volume. The reformer control volume is comprised of a biogas clean up system, heater(s)/reformer and an equipment for mixing anode exit gas (line 15 (I)) for system I, water (line 15 (II)) for system II or air ((line 15 (III)) for system III with the biogas stream. In the clean up system, the contaminants in the biogas are reduced to acceptable levels to avoid damaging the anode and/or reformer catalysts. The most attractive method to remove H_2S from the biogas is through the use of an activated carbon bed maintained at temperature 20–25 °C under atmospheric pressure. This method has been proven to be very effective (98% removal) at relatively low loadings of H_2S (<200 ppm) [35–37]. In the case of high H_2S content, additional H_2S removal technologies are required to reduce the H_2S content to below 200 ppm prior to the carbon bed. A similar absorption bed can also be used to remove silicon compounds [19] that may cause significant deactivation of the anode catalysts.

The effects of the boiler feedwater pump and the biogas blower on the overall system efficiency and exergy destruction of the system are assumed to be negligible.

Table 5
The results obtained from the computer simulation for the studied SOFC systems.

Parameter	System I	System II	System III
Generated AC electricity (MW)	2.92	2.78	2.14
Generated heat (MW)	2.33	2.14	3.21
Electrical efficiency (%)	45.1	43.0	33.0
CHP efficiency (%)	84.1	78.6	86.8
Total exergy destruction of the system (MW)	3.61	3.78	4.28
Number of cells in the SOFC stack (–)	102,863	87,614	93,726
Flow rate of the produced hot water (kg s^{-1})	10.10	9.23	13.89
Heat transfer from the SOFC stack (kW)	43.3	39.0	40.1
Reforming agent to the inlet biogas ratio (kg kg^{-1})	0.93	0.38	1.38

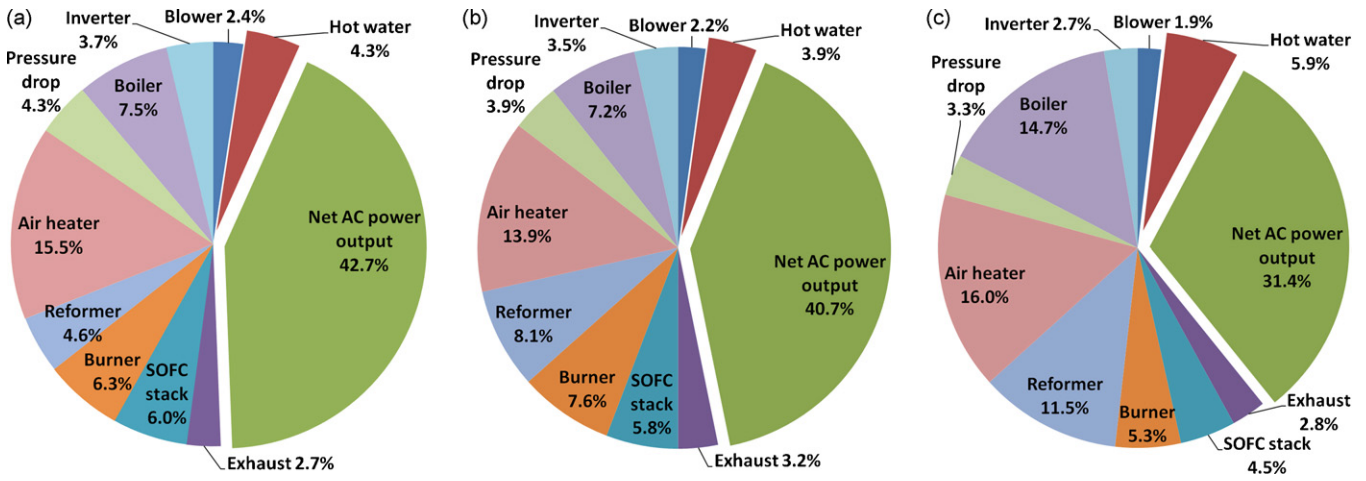

Fig. 4. The share of each component in exergy destruction of the input biogas to the (a) system I with AGR, (b) system II with SR, and (c) system III with POX.

4. Computer simulation

To evaluate the performance of the biogas-fuelled SOFC systems shown in Fig. 2, a computer code developed by the authors for the simulation of planar SOFCs at cell, stack and system levels was used. A detailed model of the cell including the electrochemical reactions (R1) and (R2) in anode and cathode, respectively, and steam reforming and water gas shift reactions (R3) and (R4) in anode was considered in the computer code to determine the activation, ohmic, and concentration polarizations. The modeling of polarizations used in the computer code has been described in Refs. [38–40]. The inlet and outlet fuel streams from the anode were assumed to be in thermodynamic equilibrium in the cell modeling

$$H_2 + O^{2-} \rightarrow H_2O + 2e^- \quad (R1)$$

$$1/2O_2 + 2e^- \rightarrow O^{2-} \quad (R2)$$

$$CH_4 + H_2O \leftrightarrow CO + 3H_2 \quad (R3)$$

$$CO + H_2O \leftrightarrow CO_2 + H_2 \quad (R4)$$

The SOFC stack model used in the computer code is the extension of the cell model by taking account of the heat transfer from the stack. Since heat transfer from the SOFC stack affects the cell performance, an appropriate insulation system to control the heat transfer was used. The insulation system considered in this study consists of an insulation layer mechanically supported by two metal layers. To determine the rate of heat transfer from the SOFC stack, conductive heat transfer in the insulation layer and radiation and natural convective heat transfer from the outer metal layer were taken into account. The effect of heat transfer from the SOFC stack on the cell performance was finally considered in the computer code. A 2% voltage drop in the SOFC stack was also assumed in this study.

The balance of plant (BoP) components such as the heater, blower, and burner was thermodynamically modeled under steady state operating conditions. The properties, composition and flow rate of all streams in the system are determined after modeling the BoP components. Finally, the net electric power, generated heat, total exergy destruction of the system, electrical and CHP efficiencies can be determined from Eqs. (1)–(5), respectively

$$\dot{W}_{\text{net electric}} = \dot{W}_{\text{SOFC stack}} - \dot{W}_{\text{blower}} \quad (1)$$

$$\dot{Q} = \dot{m}_{\text{water}}(h_{\text{hot water}} - h_{\text{cold water}}) \quad (2)$$

$$\dot{E}x_{\text{destruction,total}} = \dot{E}x_{\text{biogas}} - \dot{W}_{\text{SOFC stack}} - (\dot{E}x_{\text{hot water}} - \dot{E}x_{\text{cold water}}) \quad (3)$$

$$\eta_{\text{electric}} = \frac{\dot{W}_{\text{net electric}}}{\dot{m}_{\text{biogas}}\ \text{LHV}_{\text{biogas}}} \quad (4)$$

$$\eta_{\text{CHP}} = \frac{\dot{W}_{\text{net electric}} + \dot{Q}}{\dot{m}_{\text{biogas}}\ \text{LHV}_{\text{biogas}}} \quad (5)$$

where, $\dot{W}$, $\dot{Q}$, $\dot{E}x$, $\dot{m}$, h, LHV, and η represent the electric power, generated heat, exergy, mass flow rate, specific enthalpy, lower heating value, and efficiency, respectively. In the system modeling, heat transfer from the air heater, reformer, burner, and boiler was not considered in the calculations.

The minimum required flow rate of anode gas recirculation for system I, water for system II and air for system III to prevent carbon deposition over the anode catalyst is determined after finding the carbon deposition boundary based on the thermodynamic equilibrium assumption. The carbon deposition boundary is determined considering that the solid carbon can be formed by the three reactions of carbon decomposition (R5) [41], CO reduction (R6) and the Boudouard reaction (R7) [31].

$$CH_4 \leftrightarrow C + 2H_2 \quad (R5)$$

$$CO + H_2 \leftrightarrow C + H_2O \quad (R6)$$

$$2CO \leftrightarrow C + CO_2 \quad (R7)$$

To validate the computer code in cell level, the performance of ASC 3 anode-supported cells, produced by H.C. Strack Company was simulated [42]. As shown in Fig. 3, the cell performance predicted by the computer code shows a satisfactory agreement with the experimental data at the cell operating temperatures of 700 and 800 °C.

The input data used for the evaluation of the SOFC cell, stack, and balance of plant are listed in Tables 2–4. The anode-supported ASC 3 cell is used in the computer simulation, comprised of Ni/YSZ (yttrium stabilized zirconia) anode, dense YSZ electrolyte and YSZ/LSM (lanthanum strontium manganese oxide) cathode. The porosity and tortuosity of electrodes are assumed to be 0.33 and 4, respectively.

The Robert O. Pickard Centre's WWTP is selected as a plant studied to evaluate the SOFC systems. This plant treats approximately 450,000 $m^3\ day^{-1}$ domestic, commercial and industrial wastewater in the city of Ottawa. Prior to 1992, the biogas produced in the plant was burned and flared off into the atmosphere. From 1992 to 1997, the biogas was burned in boilers to produce hot water for space heating of the plant and the AD process temperature control. During low heat demand periods, the hot water was discharged into the sewer, wasting potentially useful energy. In

1998, a conventional CHP system was installed in the plant. This system converts 32% of the chemical energy of the produced biogas into electricity and 48% into heat. In the conventional CHP system, the biogas is burned in three engines driving generators to produce the electricity required for aeration blowers and centrifuges in the AD process. The generated heat is found to be more than enough to meet the heat demand in summer for the WWTP [43].

5. Results and discussion

Table 5 shows the computer simulation results based on the cell, stack and system input data given in Tables 2–4. According to this table, the electrical efficiency of the SOFC systems investigated is higher than that of the conventional CHP system being operated in the Pickard Plant. Among the studied SOFC systems, system I with the anode gas recirculation exhibits the maximum electrical efficiency of 45.1% that is 13.1% higher than that of the existing system. The electrical efficiency of system II with a steam reforming fuel processor is also 11% higher than that of the existing system. The computer simulation using the composition of the biogases produced in WWTPs in Ontario provides similar results. Indeed, in case of operating system I or system II at any WWTP in Ontario, it is expected that the generated electricity is greater than the amount required to operate the plant and the extra generated electricity can be sold to the electrical grid.

The computer simulation of system III with the partial oxidation fuel processor provides the highest CHP efficiency among the three studied SOFC systems. Since the heat generated from systems I or II is enough for a WWTP, the high CHP efficiency of system III may not be important for this application. The advantage of system II compared to the other studied systems is the number of cells required for the SOFC stack. The number of cells for system II is 17.4% less than that for system I.

Overall, it seems systems I and II are more suitable to be applied in WWTPs; however, a detailed economic analysis would be required for selecting the best system for this application.

5.1. Exergy analysis

Fig. 4 shows the share of each component in exergy destruction of the input biogas fuel to the systems studied. The exergy destruction in SOFC stack are not as significant as the exergy destruction in the air heater, reformer or boiler, because the heat generated due to polarizations in a high temperature cell can be used for generating more electricity in other power generation systems. In all the studied systems, the air heater has the largest share in exergy destruction of the input biogas, followed by the boiler and burner for system I, reformer and burner for system II, and boiler and reformer for system III. There is a considerable potential to generate more electricity in all the studied systems, especially in system III, if they are combined with other power generation systems and appropriately optimized using pinch technology and exergy analysis [44,45].

5.2. Sensitivity analysis

The effect of the fuel utilization ratio, temperature of the inlet fuel and air to the SOFC stack, and the cell operating voltage on the electrical and CHP efficiencies, the generated electricity and heat, the total exergy destruction, and the number of cells in the SOFC stack was studied through a detailed sensitivity analysis. Except the operating parameter studied in the sensitivity analysis all other parameters are fixed and based on Tables 2–4.

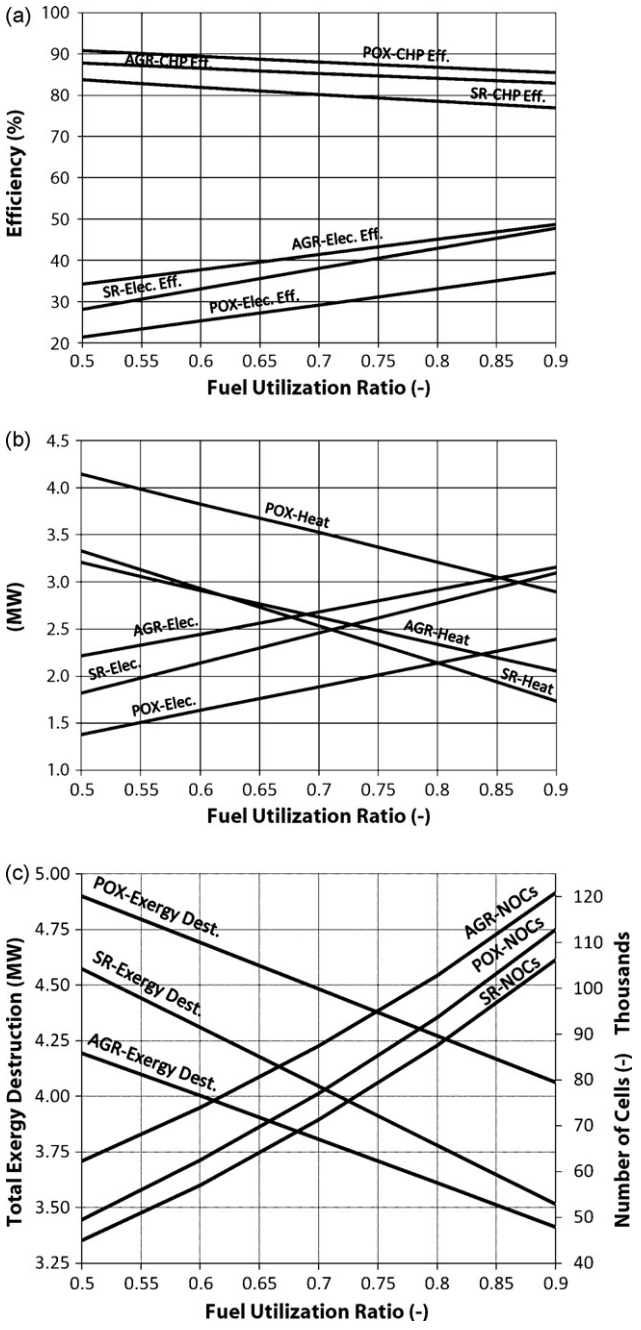

Fig. 5. Effect of the fuel utilization ratio on the (a) electrical and CHP efficiencies (b) electricity and heat generated and (c) total exergy destruction and number of cells, in system I with AGR, system II with SR and system III with POX.

5.2.1. Effects of the fuel utilization ratio

As shown in Fig. 5a, the increase in the fuel utilization ratio leads to a linear increase in the electrical efficiency and a linear decrease in the CHP efficiency of all the studied systems. For the investigated range of the fuel utilization ratios, the electrical efficiency of systems I and III are found to be the highest and lowest, respectively, whereas system III provides the highest CHP efficiency among the studied systems. The electrical efficiency of system II approaches to that of system I as the fuel utilization ratio increases. Fig. 5b shows that the amount of electricity generated in systems I and II is higher than the heat generated in those systems once the fuel utilization ratio exceeds 69% for system I and 72% for system II. In the entire range of the fuel utilization ratios investigated, the generated heat is greater than the generated electricity in system III. According

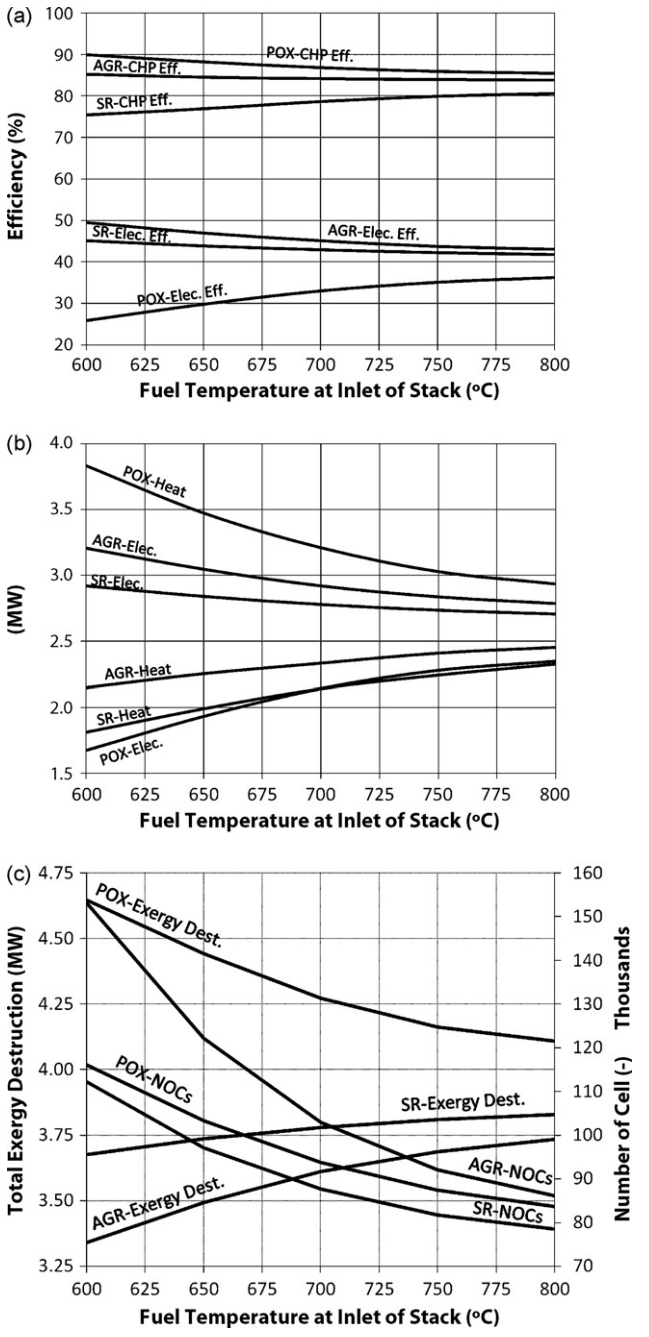

Fig. 6. Effect of the inlet fuel temperature to the SOFC stack on the (a) electrical and CHP efficiencies (b) electricity and heat generated and (c) total exergy destruction and number of cells, in system I with AGR, system II with SR and system III with POX.

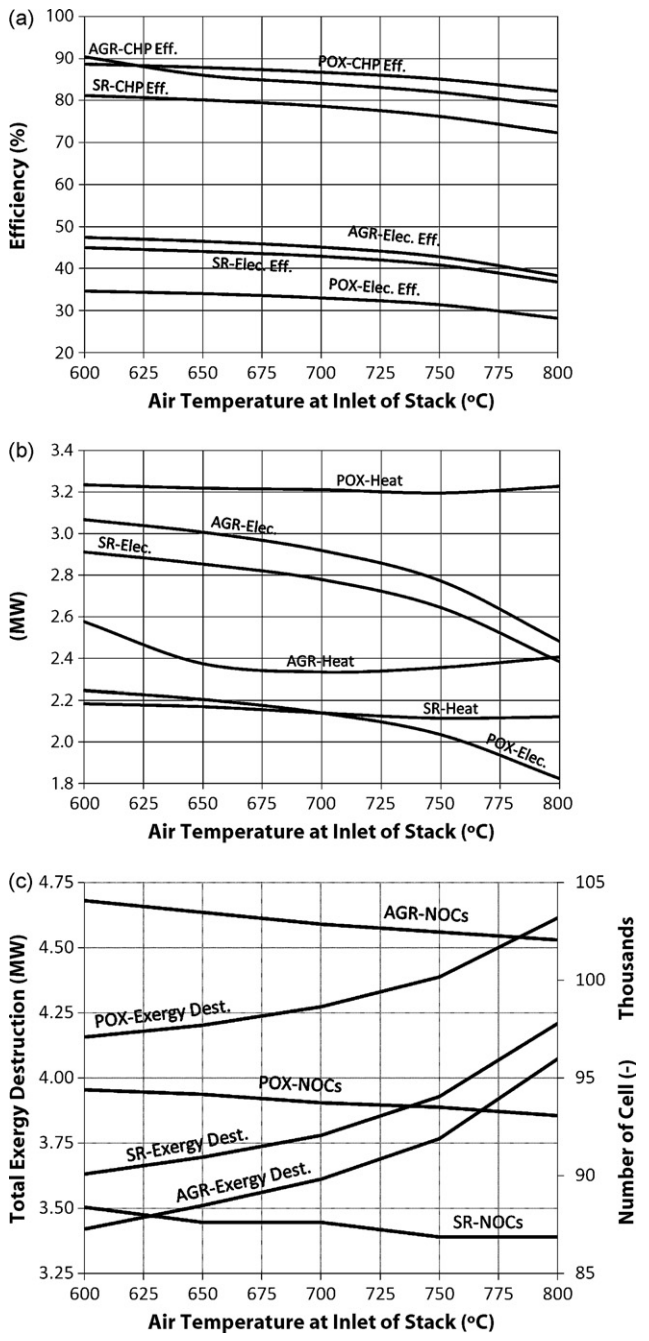

Fig. 7. Effect of the inlet air temperature to the SOFC stack on the (a) electrical and CHP efficiencies (b) electricity and heat generated and (c) total exergy destruction and number of cells, in system I with AGR, system II with SR and system III with POX.

to Fig. 5c, the total exergy destruction in system III is the highest among the studied systems, followed by systems II and I. The increase in the fuel utilization ratio leads to a linear decrease in the total exergy destruction and a progressive increase in the number of cells in SOFC stack of all the studied systems. Accordingly, the size and initial investment cost of the SOFC stack increases with increasing the fuel utilization ratio. For the investigated range of the fuel utilization ratios, the SOFC stack in system I has the highest number of cells, followed by systems III and II.

5.2.2. Effects of the fuel temperature at the inlet of the SOFC stack

As shown in Fig. 6a and b, the electrical efficiency and the electricity generated in systems I and II decrease (unlike system III) with increasing the fuel temperature at the inlet of the SOFC stack. For the investigated range of the inlet fuel temperature at the SOFC stack, the electrical efficiency of system I and the CHP efficiency of system III are the highest among the studied systems. In this range, the electricity generated in systems I and II are greater than the generated heat. According to Fig. 6c, the total exergy destruction in system I is the lowest among the studied systems, followed by systems II and III. The increase in the fuel temperature leads to an increase in the total exergy destruction in systems I and II; however, this value decreases in system III. Increasing the fuel temperature at the inlet of the SOFC stack has a significant effect to decrease the number of cells in all the studied systems, especially in system I; however, this effect reduces at high inlet fuel tem-

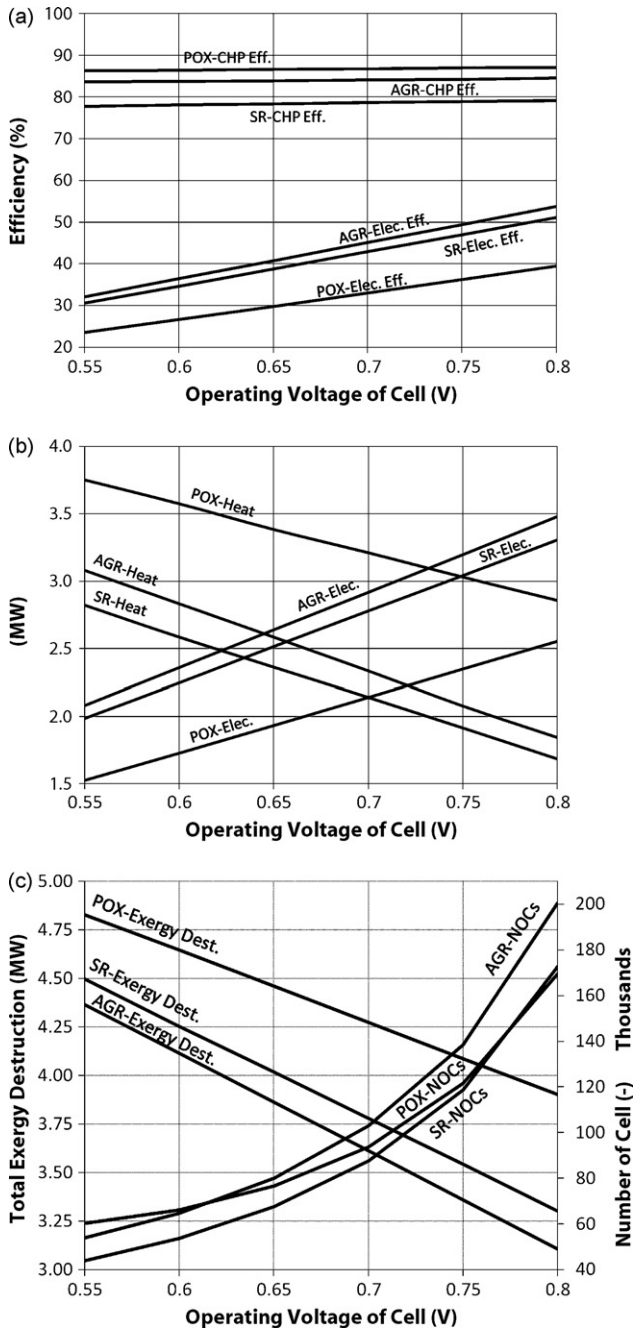

Fig. 8. Effect of the cell operating voltage on the (a) electrical and CHP efficiencies (b) electricity and heat generated and (c) total exergy destruction and number of cells, in system I with AGR, system II with SR and system III with POX.

peratures. Therefore, by increasing the fuel temperature, the size and initial investment cost of the SOFC stack decreases for all the studied systems.

5.2.3. Effects of the air temperature at the inlet of the SOFC stack

Fig. 7a and b shows that the electrical and CHP efficiencies and the electricity generated in all the studied systems decrease with increasing the air temperature at the inlet of the SOFC stack. At air temperatures below 620 °C, the CHP efficiency of system I is more than that of systems II and III. Unlike system III, the electricity generated in systems I and II are higher than the generated heat in the investigated range of the inlet air temperature. As seen in Fig. 7c, the total exergy destruction in system III is the highest, followed by systems II and I. The increase in the air temperature leads to a progressive increase in the total exergy destruction and a linear decrease in the number of cells in SOFC stack for all the studied systems.

5.2.4. Effects of the cell operating voltage

As shown in Fig. 8a and b, the electrical efficiency and the electricity generated increase significantly with increasing the cell operating voltage in all the studied systems. However, the heat generated decreases with increasing the cell operating voltage and the CHP efficiency is relatively constant in all the studied systems at the investigated range of the cell voltages. The generated heat is greater than the generated electricity in system III, although the electricity generated in systems I and II are higher than the generated heat once the operating voltage of a cell exceeds 0.65 V for system I and 0.64 V for system II. The total exergy destruction in system III is the highest among the studied systems, followed by systems II and I (Fig. 8c). The increase in the cell operating voltage leads to a linear decrease of the total exergy destruction and a progressive increase of the number of cells in SOFC stack of all the studied systems. Therefore, the size and initial investment cost of the SOFC stack for all the studied systems increases with increasing the cell operating voltage. When the cell operating voltage exceeds 0.6 V, the SOFC stack in system I has the highest number of cells among the studied systems. For the cell operating voltage less than 0.78 V, the number of cells in system II is the lowest among the studied systems.

6. Conclusions

The produced biogas is found to be suitable for SOFC systems as the high amount of carbon dioxide present in the gas can reduce the required amount of the anode gas recirculation for system I, water for system II, and air for system III. When the biogas produced in a WWTP is used in an SOFC system with anode gas recirculation or steam reforming fuel processor, the electricity and heat required to operate the plant can be completely self-supplied and the extra electricity generated can be sold to the electrical grid.

Among the SOFC systems studied, system I exhibits an electrical efficiency of 45.1%, followed by systems II and III with an electrical efficiency of 43% and 33%, respectively. The number of cells required for the SOFC stack is the lowest for system II, which is around 17.4% less than that for system I. There is a considerable potential to generate more electricity in all the studied systems, especially in system III, if they are combined with other power generation system and appropriately optimized. According to the sensitivity analysis conducted in this study, increasing the fuel utilization ratio and the cell operating voltage and decreasing the inlet air temperature to the SOFC stack lead to an increase in the electrical efficiency, the number of cells in SOFC stack, and the amount of electricity generated in the systems studied. Overall, systems I and II are found to be more suitable to be used in WWTPs than system III; however, a detailed economic analysis is required for selecting the best system for this application.

Acknowledgments

The authors gratefully acknowledge financial support provided by NSERC of Canada, EcoEnergy Technology Initiative Program, and AAFC-NRC Bioproducts Program.

References

[1] S. Gair, A. Cruden, J. McDonalda, T. Hegarty, M. Chesshire, J. Power Sources 154 (2006) 472–478.
[2] S. Trogisch, J. Hoffmann, L. Daza Bertrand, J. Power Sources 145 (2005) 632–638.
[3] J.V. herle, Y. Membrez, O. Bucheli, J. Power Sources 127 (2004) 300–312.
[4] S.T. Naumann, C. Myrkn, J. Power Sources 56 (1995) 45–49.
[5] R. Bove, P. Lunghi, J. Power Sources 145 (2005) 588–593.

[6] R.J. Spiegel, J.L. Preston, Waste Manage. 23 (2003) 709–717.
[7] National Fuel Cell Research Center, U of California, Irvine, www.nfcrc.uci.edu (accessed 12.12.08).
[8] M. Krumbeck, T. Klinge, B. Doding, J. Power Sources 157 (2006) 902–905.
[9] I.V. Yentekakis, J. Power Sources 160 (2006) 422–425.
[10] I.V. Yentekakis, T. Papadam, G. Goula, Solid State Ion. 179 (2008) 1521–1525.
[11] G. Goula, V. Kiousis, L. Nalbandian, I.V. Yentekakis, Solid State Ion. 177 (2006) 2119–2123.
[12] Y. Shiratori, K. Sasaki, J. Power Sources 180 (2008) 738–741.
[13] Y. Shiratori, T. Oshima, K. Sasaki, Int. J. Hydrogen Energy 33 (2008) 6316–6321.
[14] Y. Yi, A.D. Rao, J. Brouwer, G.S. Samuelsen, J. Power Sources 144 (2005) 67–76.
[15] L. Appels, J. Baeyens, J. Degreve, R. Dewil, Prog. Energy Combust. Sci. 34 (2008) 755–781.
[16] M.H. Gerardi, The Microbiology of Anaerobic Digesters, first ed., Wiley, NJ, 2003.
[17] D. Deublein, A. Steinhauser, Biogas from Waste and Renewable Resources, first ed., Wiley–VCH, Weinheim, 2008.
[18] R.M. Jingura, R. Matengaifa, Renew. Sustain. Energy Rev. 13 (2009) 1116–1120.
[19] I. Wheeldon, C. Caners, K. Karan, B. Peppley, Int. J. Green Energy 4 (2007) 221–231.
[20] D. Singh, E. Hernandez-Pacheco, P.N. Hutton, N. Patel, M.D. Mann, J. Power Sources 142 (2005) 194–199.
[21] A.L. Dicks, J. Power Sources 71 (1998) 111–122.
[22] S. Assabumrungrat, N. Laosiripojana, V. Pavarajarn, W. Sangtongkitcharoen, A. Tangjitmatee, P. Praserthdam, J. Power Sources 139 (2005) 55–60.
[23] W. Sangtongkitcharoen, S. Assabumrungrat, V. Pavarajarn, N. Laosiripojana, P. Praserthdam, J. Power Sources 142 (2005) 75–80.
[24] T. Takeguchi, Y. Kani, T. Yano, R. Kikuchi, K. Eguchi, K. Tsujimoto, Y. Uchida, A. Ueno, K. Omoshiki, M. Aizawa, J. Power Sources 112 (2002) 588–595.
[25] T. Horita, K. Yamaji, T. Kato, H. Kishimoto, Y. Xiong, N. Sakai, M.E. Brito, H. Yokokawa, J. Power Sources 145 (2005) 133–138.
[26] L.E. Arteaga, L.M. Peralta, V. Kafarov, Y. Casas, E. Gonzales, Chem. Eng. J. 136 (2008) 256–266.
[27] R.J. Braun, S.A. Kleina, D.T. Reindla, J. Power Sources 158 (2) (2006) 1290–1305.
[28] S.H. Chan, O.L. Ding, Int. J. Hydrogen Energy 30 (2005) 167–179.
[29] P. Piroonlerkgul, S. Assabumrungrat, N. Laosiripojana, A.A. Adesina, Chem. Eng. J. 140 (2008) 341–351.
[30] N. Hotz, S.M. Senn, D. Poulikakos, J. Power Sources 158 (2006) 333–347.
[31] S. Farhad, F. Hamdullahpur, J. Power Sources 191 (2009) 407–416.
[32] V. Modafferi, G. Panzera, V. Baglio, F. Frusteri, P.L. Antonucci, Appl. Catal. A: Gen. 334 (2008) 1–9.
[33] S. Farhad, F. Hamdullahpur, J. Power Sources 193 (2009) 632–638.
[34] R. Peters, E. Riensche, P. Cremer, J. Power Sources 86 (2000) 432–441.
[35] R.J. Spiegel, J.L. Preston, J. Power Sources 86 (2000) 283–328.
[36] R. Yan, D.T. Liang, L. Tsen, J.H. Tay, Environ. Sci. Technol. 36 (2002) 4460–4466.
[37] S.M. Zicari, Removal of hydrogen sulfide from biogas using cow-manure compost, M.Sc. Thesis, Cornell University, 2003.
[38] S.H. Chan, K.A. Khor, Z.T. Xia, J. Power Sources 93 (2001) 130–140.
[39] A.V. Virkar, J. Chen, C.W. Tanner, J. Kim, Solid State Ion. 131 (2000) 189–198.
[40] J.W. Kim, A.V. Virkar, K.Z. Fung, K. Mehta, S.C. Singhal, J. Electrochem. Soc. 146 (1) (1999) 69–78.
[41] M. Younessi-Sinaki, E.A. Matida, F. Hamdullahpur, Int. J. Hydrogen Energy 34 (9) (2009) 3710–3716.
[42] H.C. Strack Company, www.hcstarck-ceramics.com/ (accessed April 2009).
[43] S. Farhad, Y. Yoo, F. Hamdullahpur, Proceedings of the 9th International Colloquium on Environmentally Preferred Advanced Power Generation (ICEPAG-2009), CA, USA, February, 2009.
[44] S. Farhad, M. Saffar-Avval, M. Younessi-Sinaki, Int. J. Energy Res. 32 (1) (2007) 1–11.
[45] S. Farhad, M. Younessi-Sinaki, M.R. Golriz, F. Hamdullahpur, Int. J. Exergy 5 (2) (2008) 164–176.